Available online at www.sciencedirect.com
ScienceDirect
Journal of the European Ceramic Society 27 (2007) 2111–2117
www.elsevier.com/locate/jeurceramsoc

Gas/solid reaction during sintering of Si_3N_4 ceramics in an air furnace

Nirut Wangmooklang [a,*], Kuljira Sujirote [b], Supatra Jinawath [a], Shigetaka Wada [a]

[a] *Research Unit of Advanced Ceramics, Department of Materials Science, Faculty of Science, Chulalongkorn University, Bangkok 10330, Thailand*
[b] *National Metal and Materials Technology Center, Pathumthani 12120, Thailand*

Received 19 February 2006; received in revised form 18 May 2006; accepted 5 June 2006
Available online 11 September 2006

Abstract

Solid/gas reaction during sintering of Si_3N_4 ceramics in an air atmosphere was investigated. The Si_3N_4 specimens were prepared from β-powder with MgO and Al_2O_3 5 wt% each as sintering aids. The oxygen content of the mixtures after milling increased with increasing milling time. The SiO_2 content was found to cause more significant mass loss of the sintered specimens than the sintering temperature. There was also a gradient of the oxygen partial pressure (P_{O_2}) in the crucible during sintering resulting in the formation of silicon oxynitride (Si_2N_2O) on the surfaces of Si_3N_4 specimens in different quantities. The mass loss reaction, amount of mass loss as a function of soaking time and sintering temperature, mass loss difference between the top and the bottom of specimens and the formation of Si_2N_2O are discussed.

Keywords: Gas/solid reaction; Si_3N_4; Sintering

1. Introduction

Silicon nitride (Si_3N_4) ceramics have been intensively studied for many years because of their great potential for structural applications at room and elevated temperatures. These are due to their excellent mechanical properties in combination with good corrosion and thermal shock resistance.[1–3] Commercial uses for Si_3N_4 ceramics range from bearings, cutting tools and wear parts to turbocharger rotors and gas-turbine components. However, throughout this period it has been commonly accepted that Si_3N_4 ceramics are usually prepared from α-Si_3N_4 powder with some amount of sintering additives and must be sintered in N_2 atmosphere under a pressure of over 0.1 MPa, because Si_3N_4 is easily oxidized in air at high temperature or decomposed to Si (s, l) and N_2 (g) at a low P_{N_2} atmosphere.[4–6] The instability of Si_3N_4, mass loss phenomena during the sintering and the formation of the heterogeneous surface layer had been investigated experimentally.[6–12]

One of the authors studied the mass loss phenomena during sintering Si_3N_4 ceramics in a N_2 furnace.[13–15] Through the study, it was thought that Si_3N_4 could be sintered in an air atmosphere furnace. And it was realized by using a double structure of Al_2O_3 crucibles as sagger and Si_3N_4 packing powder. However, the study was preliminary and there were some reactions to be clarified.[16,18]

In this paper, gas/solid reaction during sintering of Si_3N_4 ceramics in an air atmosphere is investigated. The β-Si_3N_4 powder was used as starting material instead of usual α type powder. Based on the experimental results, the oxygen partial pressure (P_{O_2}) and gas/solid reaction during sintering of Si_3N_4 ceramics in an air furnace are discussed.

2. Experimental procedure

2.1. Materials and preparation of Si_3N_4 green bodies

β-Si_3N_4 powder (SN-F2 grade, Denki Kagaku Kogyo K.K. Co., Ltd., Japan) was used as a starting material. It included 1.18 wt% oxygen and 0.2 wt% Fe. The average particle size (D_{50}) was 29 μm. The powder was mixed and milled with 5 wt% MgO (99.9% pure, Iwatani Chemicals Co., Ltd., Japan) and 5 wt% Al_2O_3 (99.99% pure, Taimei Chemicals Co., Ltd., Japan) by attrition mill using a ZrO_2 pot and Si_3N_4 balls of 5 mm in diameter. The mixture with mixing time for 6 h in ethanol was denoted as E6h and that with mixing time for 16 h in *n*-hexane was denoted as H16h. Then, the slurry using ethanol as a solvent

* Corresponding author. Tel.: +66 9 003 6717/2 218 5555; fax: +66 2 218 5561.
E-mail address: nirutw77@yahoo.com (N. Wangmooklang).

0955-2219/$ – see front matter © 2006 Elsevier Ltd. All rights reserved.
doi:10.1016/j.jeurceramsoc.2006.06.004

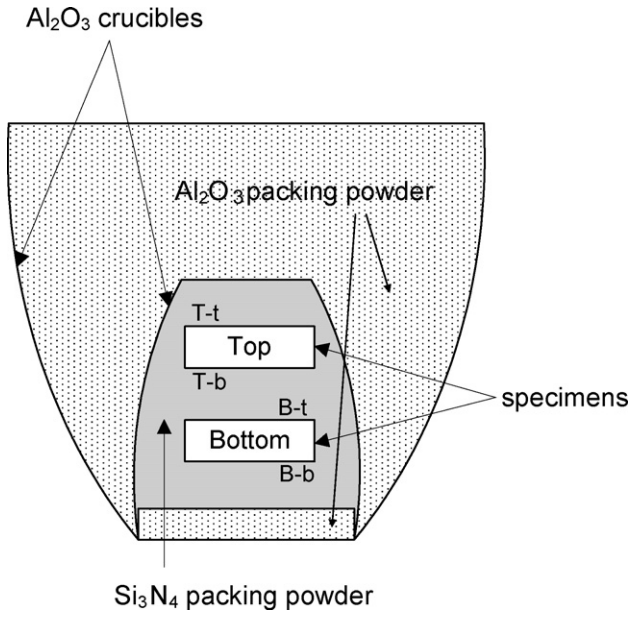

Fig. 1. Schematic of the crucible structure.

was dried at 80 °C in an oven and the slurry using *n*-hexane was first kept at room temperature until most of *n*-hexane evaporated and then dried at 100 °C in the same oven. The dried powders were sieved through a 100 mesh screen. The obtained powders were formed into tablets of 20 mm in diameter and 5 mm in thickness by mechanical pressing at 20 MPa followed by cold isostatic pressing (CIP) at 200 MPa.

2.2. Sagger structure and sintering

Two tablets of each type were placed within a powder bed of coarse Si_3N_4 powder (SN-F2, particle size >300 μm) of approximately 32 g in a high purity Al_2O_3 crucible (~40 mm inner diameter × ~36 mm height, Nikkato Co. Ltd., Japan). Then, the crucible was set in a larger Al_2O_3 crucible (~82 mm inner diameter × ~70 mm height) as shown in Fig. 1. Alumina powder (A-11 grade, Fuji Kasei Co., Ltd., Japan) of approximately 235 g was filled to the space between the two crucibles. To avoid the reaction of Si_3N_4 packing powder with the bottom of larger Al_2O_3 crucible, Al_2O_3 powder was also layered in the lower part of a small crucible. Sintering was performed in an air atmosphere furnace at a temperature ranging between 1500 °C and 1700 °C for 2 h with a heating and cooling rate of 10 °C/min.

2.3. Characterization

The particle size distributions of the powders before and after milling were measured by particle size analyzer (SA-CP2, Shimadzu, Japan). The oxygen contents of the raw Si_3N_4 powder and the powder mixtures were analyzed by an Oxygen/Nitrogen determinator (TC-436 DR, LECO, Japan). Mass loss of specimens was taken as the difference between the mass of specimens before and after sintering. Crystal phases of sintered specimens were identified by an X-ray diffractometer (D8 Advance, Bruker Co., Ltd., Germany).

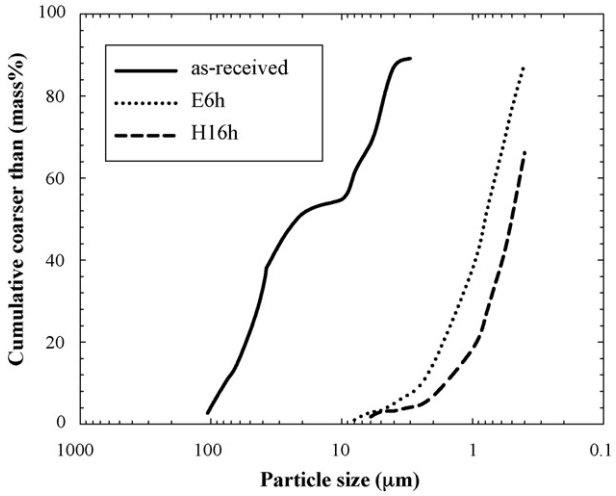

Fig. 2. Particle size distribution of as-received SN-F2 and powders after milling by attrition mill.

3. Experimental results

3.1. Properties of mixed powder after milling

The particle size distributions of the raw Si_3N_4 powder and the powders after milling are shown in Fig. 2. The attrition mill could reduce the particle size of the powder down to submicrometer size and the average particle size of the powders after milling and mixing for 6 h (E6h) and 16 h (H16h) were 0.8 μm and 0.5 μm, respectively. The oxygen contents in these powders are shown in Fig. 3. The values in Fig. 3 did not include oxygen from the oxide additives. From the results, the oxygen content increased with increasing milling time because the fractured Si_3N_4 surfaces reacted with OH^- generated from ethanol by mechanochemical reaction to form Si–O bond.[19] *n*-Hexane was used with attention to avoid oxygen increase during mixing, because *n*-hexane does not include OH^- in the molecule. Normally, the mixed powder using *n*-hexane as a medium should be dried in a vacuum rotary evaporator in order to avoid the oxidation of the Si_3N_4 powder. However, due to limited facility

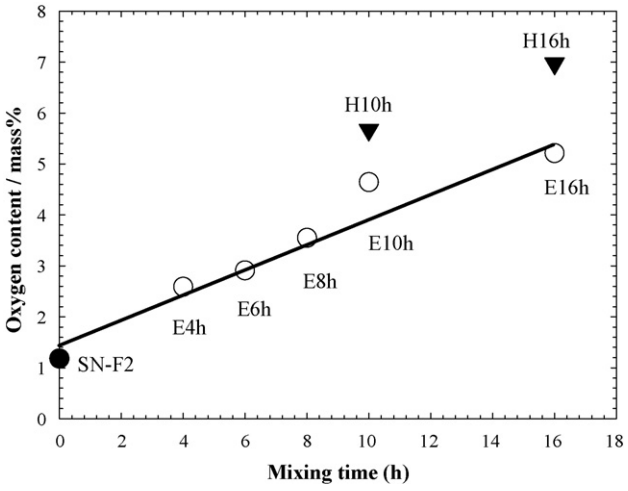

Fig. 3. Increment of oxygen content during milling as a function of milling time.

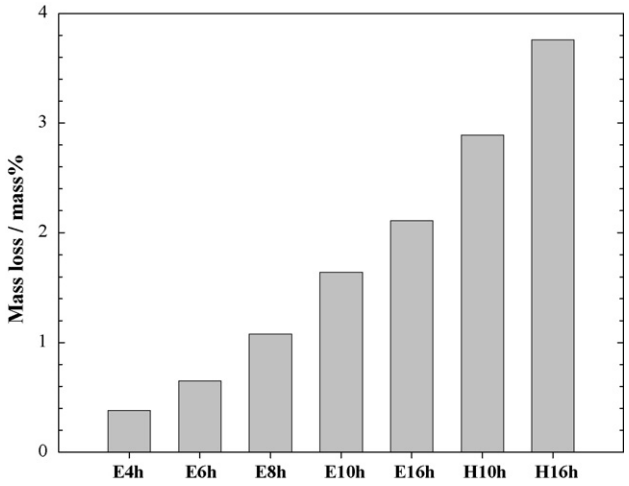

Fig. 4. Mass loss of sintered Si_3N_4 at 1700 °C for 2 h in air atmosphere as a function of oxygen content in the mixed powders.

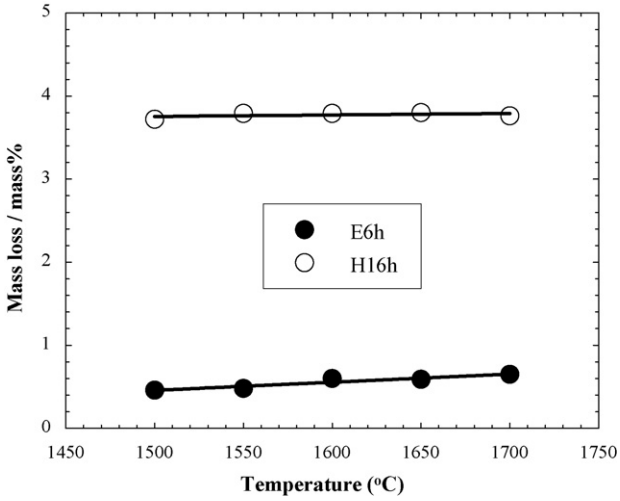

Fig. 5. Mass loss of sintered Si_3N_4 (E6h and H16h) as a function of sintering temperatures.

the slurry was dried in air as mentioned in Section 2.1. Unexpectedly, the oxygen content in the powder increased more than that in the mixture using ethanol. It was supposed that the active Si_3N_4 surface might adsorb and react with moisture during drying in air and in oven to form Si–O bond on the surface of Si_3N_4 powder.

3.2. Mass loss

The average mass loss of two specimens, top and bottom shown in Fig. 1, as a function of the oxygen content in the mixed powders is shown in Fig. 4. The mass loss significantly increased with the oxygen content in the sintered specimen. It was easily understood by comparing Fig. 3 with Fig. 4. From this viewpoint, it was thought that the mechanism was similar to that of sintering in N_2 atmosphere, where Si_3N_4 powder reacts with SiO_2 and formed SiO (g). The main reaction leading to mass loss of specimen during sintering is equated as reaction (1).[13–15,17]

$$Si_3N_4\,(s) + 3SiO_2\,(s, l) \rightarrow 6SiO\,(g) + 2N_2\,(g) \quad (1)$$

Fig. 5 shows the average mass loss of E6h and H16h as a function of sintering temperature. The mass losses did not significantly change with the sintering temperature, unlike the mass loss of Si_3N_4 ceramics sintered in N_2 atmosphere which increased with increasing the sintering temperature.[13–15]

Fig. 6(a) shows the mass loss of each specimen of E6h, top and bottom, as a function of sintering temperature. The mass loss of the top specimen in the crucible was higher than that of the bottom one. The tendency was the same for H16h specimens (Fig. 6(b)). It was suggested that the atmosphere or gas partial pressure at the top and the bottom positions of the crucible is different. Moreover, the mass loss did not increase as much with prolonging soaking time. The densities of the specimens sintered at ≥1600 °C for 2 h were almost full density, ~96–98% of theoretical density. The details concerning with some properties of the sintered bodies will be reported in the further paper.

3.3. Reaction taking place in packing powder

After sintering at 1700 °C, the Al_2O_3 packing powder at the bottom of the crucible was hardened and became a solid slab as shown in Fig. 7. The slab was approximately 3 mm thick and rather difficult to crush. However, the solid slab was softer and easy to be taken out from the crucible when the sintering temper-

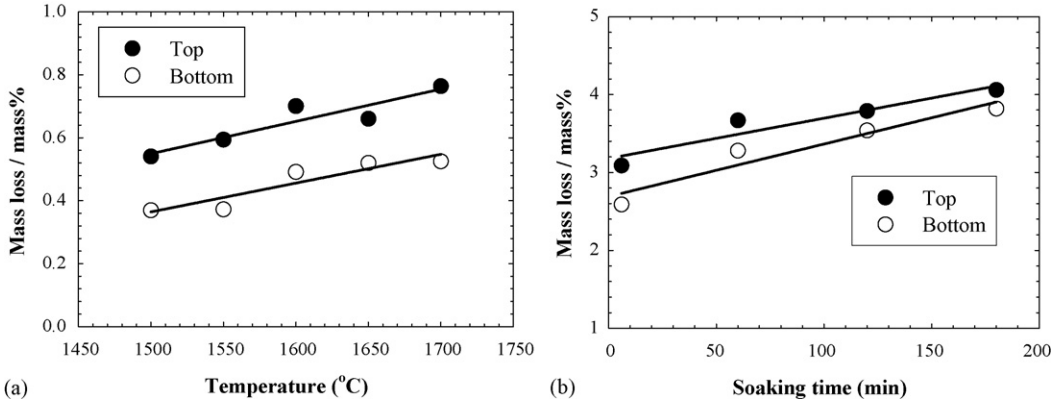

Fig. 6. Mass loss of top and bottom specimens (E6h) as a function of sintering temperature (a), and mass loss of top and bottom specimens (H16h) sintered at 1650 °C as a function of soaking time (b).

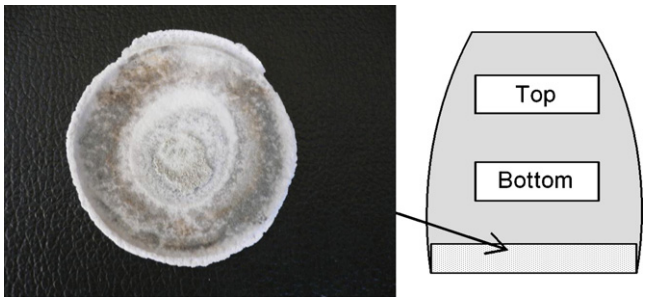

Fig. 7. Reacted Al_2O_3 packing powder (bottom side) after sintering at 1700 °C for 2 h in air atmosphere furnace.

ature was lower. The XRD profile of the slab is shown in Fig. 8. The packing powder, which was originally Al_2O_3, changed to the mixture of corundum (Al_2O_3), mullite ($3Al_2O_3{\cdot}2SiO_2$) and a small amount of amorphous phase as shown in Fig. 8. The mullite might be formed by the reaction between Al_2O_3 packing powder, SiO (g) generated from reaction (1) and/or (2) and O_2 (g) as shown in Eq. (3).

$$2Si_3N_4\,(s) + 3O_2\,(g) \rightarrow 6SiO\,(g) + 4N_2\,(g) \quad (2)$$

$$3Al_2O_3\,(s) + 2SiO\,(g) + O_2\,(g) \rightarrow 3Al_2O_3{\cdot}2SiO_2\,(s) \quad (3)$$

Amorphous phase was observed not only in the slab, but also on the edge of the small Al_2O_3 crucible. We did not analyze it, but the glassy film on the edge of the crucible might be SiO_2. We supposed that it was formed by the reaction of SiO (g) and atmospheric O_2 (g) diffused through Al_2O_3 packing powder.

Moreover, at the interface between Si_3N_4 and Al_2O_3 packing powders, a hardened layer of Si_3N_4 was formed with 1–2 mm in thickness and was easily separated from the packing powder above it. The XRD pattern of this material is shown in Fig. 9. As seen in the XRD profile, small amounts of cristobalite (SiO_2) and Si_2N_2O were observed in this layer. The formation reactions of Si_2N_2O and SiO_2 were discussed in Section 4.3.

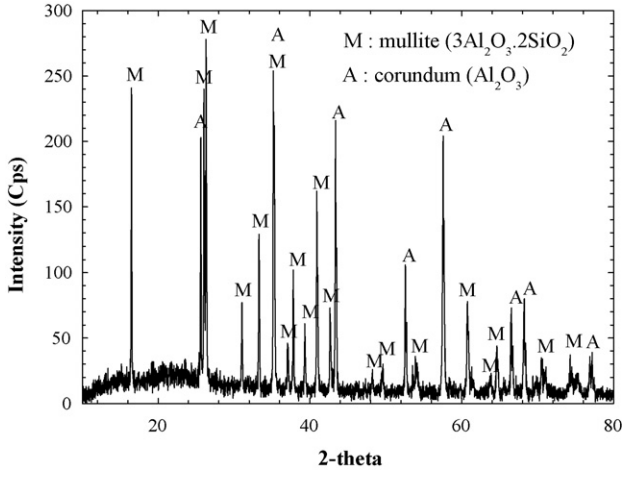

Fig. 8. XRD pattern of the reacted Al_2O_3 packing powder (bottom side) after sintering at 1700 °C for 2 h in air furnace.

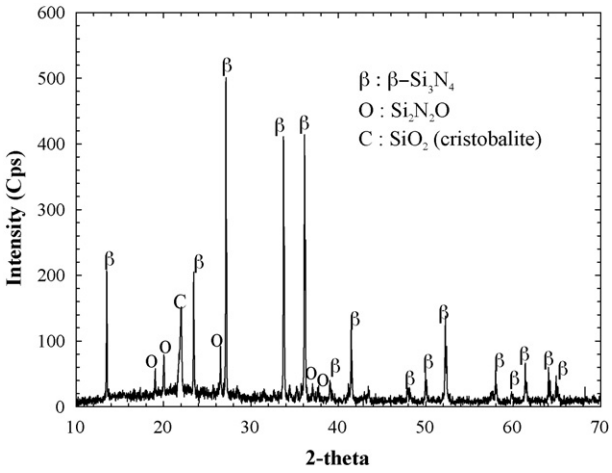

Fig. 9. XRD pattern of the reacted Si_3N_4 packing powder layer after sintering at 1700 °C for 2 h.

3.4. Crystal phase of specimens

To corroborate the reactions suggested in this work, the crystal phases of the sintered specimens and packing powder were identified by X-ray diffractometer. The XRD pattern of E6h specimen surface after sintering is shown in Fig. 10. The result indicated that the top surface of the specimen at the top position (T-t, see Fig. 1) consisted of only β-Si_3N_4 phase. On the contrary, the bottom surface of the specimen at the bottom position (B-b, see Fig. 1) consisted of only silicon oxynitride (Si_2N_2O). The surfaces T-b and B-t in Fig. 1 were composed of mixed phases of β-Si_3N_4 and Si_2N_2O. To find out the depth of Si_2N_2O, the B-b surface was ground steply and then characterized by XRD. The XRD patterns of specimen before and after grinding are shown in Fig. 11. At the depth of 47 μm, only Si_2N_2O was observed. After grinding out 75 μm, Si_2N_2O peaks reduced and β-Si_3N_4 appeared.

The effect of sintering temperature on the formation of Si_2N_2O in the specimen surfaces (B-b) was indicated by XRD patterns as shown in Fig. 12(a). β-Si_3N_4 peaks were observed at the sintering temperature of 1500 °C, their intensity gradually

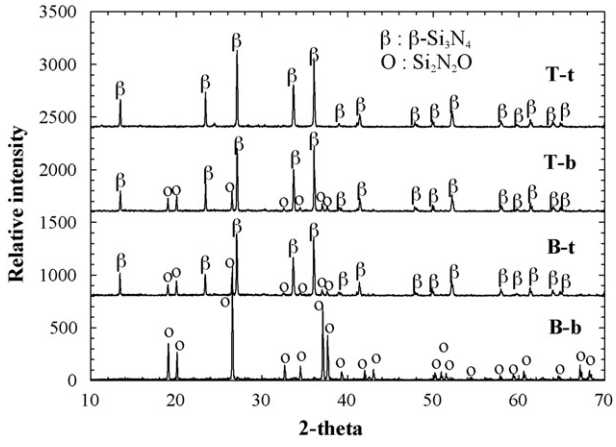

Fig. 10. XRD patterns of E6h specimen surfaces after sintering at 1700 °C for 2 h in air atmosphere furnace.

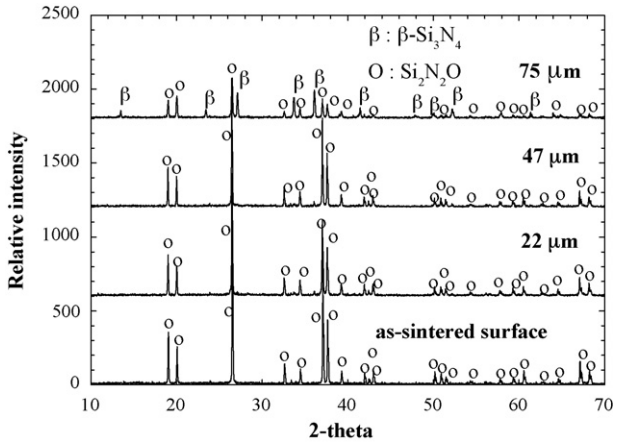

Fig. 11. XRD patterns of the specimen surface of E6h before and after grinding the bottom surface of the bottom specimen (B-b) sintered at 1700 °C for 2 h.

reduced at 1600 °C and disappeared at 1700 °C while those of Si_2N_2O clearly increased with the sintering temperature. The formation of Si_2N_2O was also favored by prolonged soaking time as indicated in Fig. 12(b), whereas β-Si_3N_4 was observed only at the shortest soaking time of 6 min, but not at 1 h and 3 h. The formation of Si_2N_2O in the surface of specimens was further discussed in Section 4.3.

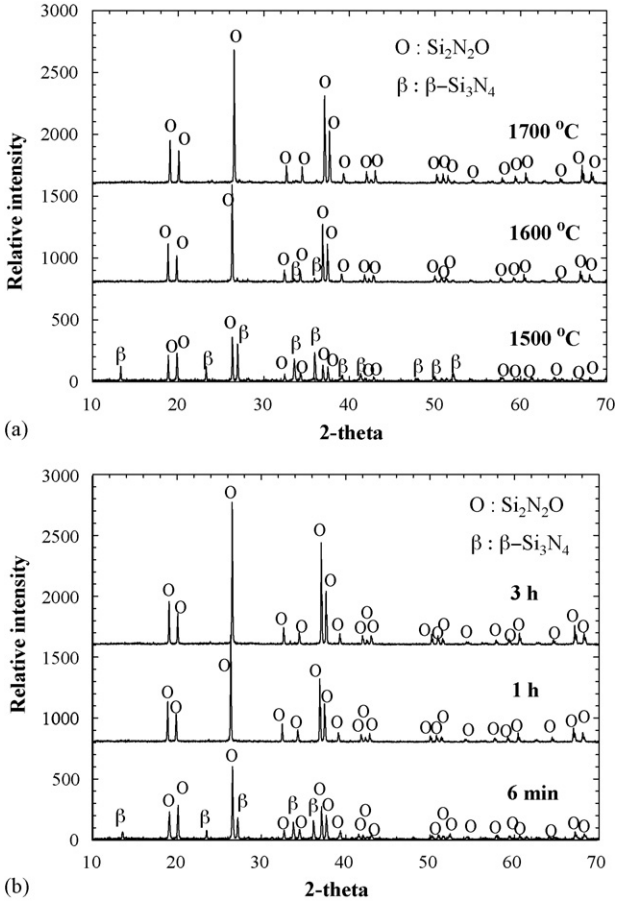

Fig. 12. XRD patterns of specimen surface (B-b) of (a) E6h sintered at 1500–1700 °C for 2 h and (b) H16h sintered at 1650 °C for various soaking times.

4. Discussion

4.1. Mass loss reaction

Materials in the small crucible are specimens of Si_3N_4 with glassy phase, Al_2O_3 packing powder, Si_3N_4 packing powder, nitrogen gas and oxygen gas. The glassy phase is composed of SiO_2, MgO and Al_2O_3. Therefore, the major mass change reactions of specimens should be through the gas/solid reactions between materials mentioned via reactions (1) and (2).

As shown in Figs. 3 and 4, the average mass loss of specimens was qualitatively proportional to the content of oxygen in the specimens. Consequently, the major mass loss reaction had to be reaction (1), nevertheless, the equilibrium P_{SiO} of reaction (2) is higher than that of reaction (1) when P_{O_2} is higher than $\sim 10^{-10}$ Pa as shown in Fig. 13(a).

Another mass loss reaction of the specimens may probably be the volatilization of MgO, which was used as sintering aid. MgO is well known to be highly volatile when used for preparing Si_3N_4 ceramics. It can vaporize to Mg (g) and O_2 (g) and/or MgO (g) at high temperature. However, we did not analyze

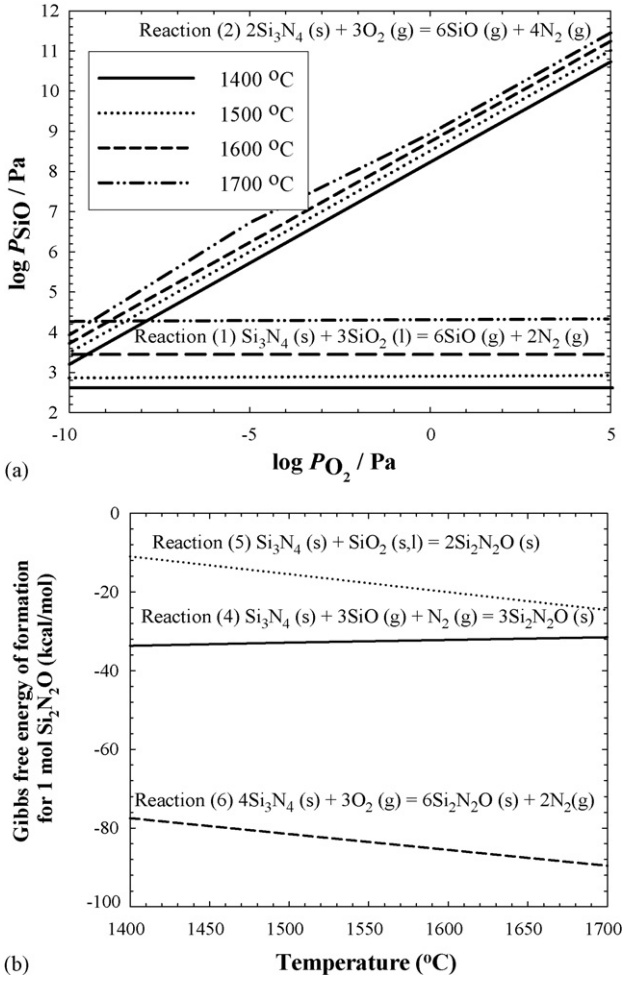

Fig. 13. (a) Equilibrium SiO (g) pressure for the reactions (1) and (2) as a function of equilibrium oxygen pressure from 1400 °C to 1700 °C and (b) Gibbs free energy of the formation of Si_2N_2O of the reactions (4)–(6) from 1400 °C to 1700 °C.

the final content of Mg(O) in the sintered specimens in this experiment.

4.2. Amount of mass loss as a function of sintering temperature and soaking time

Though the P_{SiO} of reaction (1) was independent on an oxygen partial pressure in atmosphere, it increased from 10^3 Pa at 1500 °C to 4.4×10^4 Pa at 1700 °C as shown in Fig. 13(a). Therefore, it was reasonable to assume that the mass loss should increase with increasing temperature. However, as shown in Figs. 5 and 6, the mass loss did not change so much with sintering temperature and soaking time. The independence of the mass loss on the sintering temperature and soaking time may be due to the formation of impermeable layer.

As shown in Figs. 7 and 8, Al_2O_3 packing powder in the bottom of the small Al_2O_3 crucible partially changed to mullite and SiO_2 glass layer after sintering. As explained in Section 3.3, Si_3N_4 packing powder layer adjoined to Al_2O_3 packing powder changed to Si_3N_4, Si_2N_2O and SiO_2 glass (cristobalite at room temperature) layer after sintering. This layer might soon become less permeable. The amount of gas diffused through the layer would be proportional to the total amount of SiO (g) evaporated from the reactions (1) and (2). In other words, when sintering temperature was high, the layer became impermeable in a shorter time but in a longer time at low sintering temperature. When the SiO (g) and O_2 generated from outside nearly stopped to diffuse out and in, the reaction would almost stop. As a result, mass loss was not affected by sintering temperature and soaking time by the formation of impermeable layer.

4.3. Formation of Si_2N_2O

Si_2N_2O was observed in the surface of specimens and in the Si_3N_4 packing powder adjoined to Al_2O_3 packing powder.

The formation of Si_2N_2O is only observed via a presence of liquid phase whereby the liquid phase is generally provided by the intentionally added metal oxides. The facts had already been reported by Huang et al.,[21] Mitomo et al.,[22] Ohashi et al.,[23–26] Lewis et al.,[27] Li et al.,[28] Wang et al.,[29] and Larker.[30]

Possible material balance to form Si_2N_2O is suggested as follows ((4)–(6)):

$$Si_3N_4\,(s) + 3SiO\,(g) + N_2\,(g) \rightarrow 3Si_2N_2O\,(s) \quad (4)$$

$$Si_3N_4\,(s) + SiO_2\,(s, l) \rightarrow 2Si_2N_2O\,(s) \quad (5)$$

$$4Si_3N_4\,(s) + 3O_2\,(g) \rightarrow 6Si_2N_2O\,(s) + 2N_2\,(g) \quad (6)$$

Considering the Gibbs free energies of the reactions (4)–(6) shown in Fig. 13(b), the formation of Si_2N_2O via reactions (5) and (6) is more thermodynamically favorable than reaction (4).

As discussed in Section 3.4, more amount of Si_2N_2O in sintered specimens was observed in the surface closer to the bottom side and was also in the outer surface. Therefore, the material to form Si_2N_2O in the specimen was supplied from outside of the specimen. Oxygen gas diffuses in the small Al_2O_3 crucible from outside. Then the amount of O_2 (g) was rich; in other words, oxygen partial pressure (P_{O_2}) was higher in the bottom side. Considering all facts mentioned above, the formation reaction of Si_2N_2O in the specimen might be the reaction (6).

Another possible reaction is the reaction (5), because SiO_2 (s, l) generated by the reactions (7) and (8). In these reactions, P_{O_2} affects the amount of SiO_2 (s, l) generation.

$$2SiO\,(g) + O_2\,(g) \rightarrow 2SiO_2\,(s, l) \quad (7)$$

$$Si_3N_4\,(s) + 3O_2\,(g) \rightarrow 3SiO_2\,(s, l) + 2N_2\,(g) \quad (8)$$

The SiO_2 in reaction (7) is formed by reaction between SiO (g) which generates from reaction (1) and/or (2) and O_2 (g) diffused from the atmosphere. The SiO_2 in reaction (8) is resulted from the passive oxidation of Si_3N_4. Generally, the reaction between Si_3N_4 (s) and O_2 (g) is passive oxidation when oxygen partial pressure (P_{O_2}) is high and it changes to active oxidation (reaction (2)) when $P_{O_2\,(g)}$ becomes lower. The transition condition of passive to active is affected by the atmosphere temperature and gas flowing rate.[20] However, the transition occurred at about 10^2 Pa.[14,20]

The P_{O_2} in the crucible could not be measured. Therefore, we do not know whether P_{O_2} was higher than 10^2 Pa or not in the area of specimens. As a result, it is not confident that the reaction (5) is the only one of the formation reactions of Si_2N_2O in the surface of specimens, but there will be some possibility.

In the layer of Si_3N_4 packing powder adjoined to Al_2O_3 packing powder, P_{O_2} is presumed to be high. As a result, reactions (6)–(8) occur. The SiO_2 (s, l) in reactions (7) and (8) provide a viscous glass phase for reaction (5) to generate Si_2N_2O. The glassy phase may also be formed by the reaction between SiO_2 and Al_2O_3 powder adjoined to Si_3N_4 packing powder. This liquid formation is strongly influenced by Al_2O_3 which decreases the melting temperature by forming an aluminium silicate melt. It enhances dissolution of Si_3N_4 and in this way promotes the formation of Si_2N_2O solid solution.[21]

No Si_2N_2O was generated in T-t surface and much amount of mass loss was observed because P_{O_2} was too low to precipitate SiO_2 (s, l) by reactions (7) and (8) to react with Si_3N_4. Hence, reaction (5) and/or (6) could not occur. Accordingly, the Si_3N_4 packing powder in the top part of the small sagger was easily crushed to powder and it did not include any other phase except Si_3N_4.

Plucknett and Lin sintered Si_3N_4 in air atmosphere. They observed only mass gain and generation of Si_2N_2O at the sintering temperature of 1500–1750 °C.[31] Comparing with our results, the P_{O_2} around the specimen might be higher than that of this experiment.

4.4. Mass loss difference between top and bottom specimens

As shown in Figs. 5 and 6, mass loss of the top specimen was much higher than that of bottom one. The reaction (1) is the mass loss reaction. The reactions (5) and (6) are the mass gain reaction.

The difference in the mass loss of the top and bottom specimen is sum of the mass loss and mass gain reactions. And the

mass gain reaction is affected by the P_{O_2} in the crucible as discussed in Section 4.3. However, the sequence of mass loss and mass gain reactions with soaking time is not explained exactly in this experiment.

5. Conclusions

The solid/gas reaction during sintering of Si_3N_4 ceramics in air atmosphere was investigated through the experimental data of the sintered specimens and packing powders. The following conclusions were reached.

(1) Mass loss of Si_3N_4 ceramics sintered in air significantly increased as a function of SiO_2 content in the specimen, but was less affected by the temperature change. The mass losses of the specimen placed at the top and bottom of positions in the small crucible were different due to the difference of the oxygen partial pressure during sintering. The main mass loss of Si_3N_4 specimen was due to the following reaction:

$$Si_3N_4\,(s) + 3SiO_2\,(s, l) \rightarrow 6SiO\,(g) + 2N_2\,(g)$$

(2) There was a gradient of the oxygen partial pressure (P_{O_2}) in the small crucible during sintering. The P_{O_2} at the top side of the crucible was assumed to be lower than the bottom side. This assumption was convinced by the formation of Si_2N_2O in the bottom surface of the sintered specimen, of which the content decreased inward.

Acknowledgements

This work was supported by National Metal and Materials Technology Center (MTEC) and one of the authors (N.W.) would like to thank Thailand Graduate Institute of Science and Technology (TGIST) for his scholarship.

References

1. Herrmann, H., Klemm, H. and Schubert, C., *Handbook of Ceramic Hard Materials*, *Vol. 2*. Wiley-VCH, Weinheim, Germany, 2000.
2. Kawai, C. and Yamakawa, A., Effect of porosity and microstructure on the strength of Si_3N_4: designed microstructure for high Strength, high thermal shock resistance, and facile machining. *J. Am. Ceram. Soc.*, 1997, **80**, 2705–2708.
3. Terwilliger, G. R., Properties of sintered Si_3N_4. *J. Am. Ceram. Soc.*, 1974, **57**, 48–49.
4. Batha, H. D. and Whitney, E. D., Kinetic and mechanism of the thermal decomposition of Si_3N_4. *J. Am. Ceram. Soc.*, 1973, **56**, 365–369.
5. Wada, S., Control of instability of Si_3N_4 during pressureless sintering. *J. Ceram. Soc. Jpn.*, 2001, **109**, 803–808.
6. Greskovich, C. and Prochazka, S., Stability of Si_3N_4 and liquid phase(s) during sintering. *J. Am. Ceram. Soc.*, 1981, **64**, C96–C97.
7. Lange, F. F., Volatilization associated with the sintering of polyphase Si_3N_4 materials. *J. Am. Ceram. Soc.*, 1982, **65**, C120–C121.
8. Messier, D. R. and Deguire, E. J., Thermal decomposition in the system Si–Y–Al–O–N. *J. Am. Ceram. Soc.*, 1984, **67**, 602–605.
9. Baik, S. and Raj, R., Effect of silicon activity on liquid-phase sintering of nitrogen ceramics. *J. Am. Ceram. Soc.*, 1985, **68**, C124–C126.
10. Tsuge, A., Inoue, H. and Komeya, K., Grain boundary phase crystallization of silicon nitride with material loss with heat treatment. *J. Am. Ceram. Soc.*, 1989, **72**, 2014–2016.
11. Hwang, S. L., Becher, P. E. and Lin, H. T., Desintering process in the gas pressure sintering of silicon nitride. *J. Am. Ceram. Soc.*, 1997, **80**, 329–335.
12. Lee, W. H., Kim, H. E. and Cho, S. J., Microstructure evolution of gas-pressure-sintered Si_3N_4 with Yb_2O_3 as a sintering aid. *J. Am. Ceram. Soc.*, 1997, **80**, 2737–2740.
13. Yokoyama, K. and Wada, S., Solid–gas reaction during sintering of Si_3N_4 ceramics. Part 4: mass loss reaction and morphology of Si_3N_4 ceramics. *J. Ceram. Soc. Jpn.*, 2000, **108**, 357–364.
14. Yokoyama, K. and Wada, S., Solid–gas reaction during sintering of Si_3N_4 ceramics. Part 5: mass change reaction of Si_3N_4 ceramics during sintering under N_2 gas flow in a non-carbon-element furnace. *J. Ceram. Soc. Jpn.*, 2000, **108**, 627–632.
15. Yokoyama, K. and Wada, S., Solid–gas reaction during sintering of Si_3N_4 ceramics. Part 6: suppression of mass loss reaction of Si_3N_4 ceramics during sintering. *J. Ceram. Soc. Jpn.*, 2001, **109**, 238–243.
16. Wada, S., Hattori, T. and Yokoyama, K., Sintering of Si_3N_4 ceramics in air atmosphere furnace. *J. Ceram. Soc. Jpn.*, 2001, **109**, 281–283.
17. Wada, S., Control instibility of Si_3N_4 during pressureless sintering. *J. Ceram. Soc. Jpn.*, 2001, **109**, 801–808.
18. Wada, S., Chaiyapak, P., Jinawath, S., Wasanapairnpong, T. and Yano, T., Sintering of Si_3N_4 ceramics in air atmosphere furnace (Part 2). *J. Ceram. Soc. Jpn.*, 2004, **112**, 234–237.
19. Wada, S., Increase of oxygen content in Si_3N_4 powder during ball milling using alcohol as solvent. *J. Ceram. Soc. Jpn.*, 1996, **104**, 1092–1094.
20. Wallace, L. V. and Howard, G. M., Active-to-passive transition in the oxidation of silicon carbide and silicon nitride in air. *J. Am. Ceram. Soc.*, 1990, **73**, 1540–1543.
21. Huang, Z. K., Greil, P. and Petzow, G., Formation of silicon oxynitride from Si_3N_4 and SiO_2 in the presence of Al_2O_3. *Ceram. Int.*, 1984, **10**, 14–17.
22. Mitomo, M. *et al.*, Effect of atmosphere on the reaction sintering of Si_2N_2O. *Ceram. Int.*, 1989, **15**, 345–350.
23. Ohashi, M. *et al.*, Nucleation control for hot-working of Si_2N_2O based ceramics. *J. Mater. Res.*, 1999, **14**, 170–177.
24. Ohashi, M. *et al.*, Processing, mechanical properties, and oxidation behavior of oxynitride ceramics. *J. Am. Ceram. Soc.*, 1991, **74**, 109–114.
25. Ohashi, M. *et al.*, Factors affecting mechanical properties of silicon oxynitride ceramics. *Ceram. Int.*, 1997, **23**, 27–37.
26. Ohashi, M. *et al.*, Effect of additives on some properties of silicon oxynitride ceramics. *J. Mater. Sci.*, 1991, **26**, 2608–2614.
27. Lewis, M. H. *et al.*, Pressureless-sintered ceramics based on the compound Si_2N_2O. *Mater. Sci. Eng.*, 1985, **71**, 87–94.
28. Li, Y. L. *et al.*, Reaction and formation of crystalline silicon oxynitride in Si–O–N systems under solid high pressure. *J. Am. Ceram. Soc.*, 2001, **84**, 875–877.
29. Wang, C. *et al.*, Nucleation and growth of silicon oxynitride grains in a fine-grained silicon nitride matrix. *J. Am. Ceram. Soc.*, 1998, **81**, 1125–1132.
30. Larker, R., Reaction sintering and properties of silicon oxynitride densified by hot isostatic pressing. *J. Am. Ceram. Soc.*, 1992, **75**, 62–66.
31. Plucknett, K. P. and Lin, H. T., Sintering silicon nitride ceramics in air. *J. Am. Ceram. Soc.*, 2005, **88**, 3538–3541.